



Can oxygen vacancies in ceria surfaces be measured by O1s photoemission spectroscopy?

Downloaded from: <https://research.chalmers.se>, 2025-12-04 23:28 UTC

Citation for the original published paper (version of record):

Bosio, N., Schaefer, A., Grönbeck, H. (2022). Can oxygen vacancies in ceria surfaces be measured by O1s photoemission spectroscopy?. Journal of physics. Condensed matter : an Institute of Physics journal, 34(17). <http://dx.doi.org/10.1088/1361-648X/ac4f7b>

N.B. When citing this work, cite the original published paper.

PAPER • OPEN ACCESS

Can oxygen vacancies in ceria surfaces be measured by O1s photoemission spectroscopy?

To cite this article: Noemi Bosio *et al* 2022 *J. Phys.: Condens. Matter* **34** 174004

View the [article online](#) for updates and enhancements.

You may also like

- [Enhancement of ferromagnetism in C ion implanted CeO₂ thin films](#)
Pawan Kumar, F Chand and K Asokan
- [Theoretical Study of Oxygen Vacancy Formation at LSC/GDC Interface](#)
Takayoshi Ishimoto, Kenji Sato and Michihisa Koyama
- [Development of Xe and Kr empirical potentials for CeO₂, ThO₂, UO₂ and PuO₂, combining DFT with high temperature MD](#)
M W D Cooper, N Kuganathan, P A Burr *et al.*



IOP | ebooks™

Bringing together innovative digital publishing with leading authors from the global scientific community.

Start exploring the collection—download the first chapter of every title for free.

Can oxygen vacancies in ceria surfaces be measured by O 1s photoemission spectroscopy?

Noemi Bosio^{1,2,*}, Andreas Schaefer^{2,3}  and Henrik Grönbeck^{1,2,*} 

¹ Department of Physics, Chalmers University of Technology, SE-41296 Göteborg, Sweden

² Competence Centre for Catalysis, Chalmers University of Technology, SE-41296 Göteborg, Sweden

³ Department of Chemistry and Chemical Engineering, Chalmers University of Technology, SE-41296 Göteborg, Sweden

E-mail: bosio@chalmers.se and ghj@chalmers.se

Received 15 October 2021, revised 5 January 2022

Accepted for publication 27 January 2022

Published 25 February 2022



Abstract

X-ray photoemission spectroscopy is a standard technique for materials characterization and the O 1s binding energy is commonly measured for oxides. Here we use density functional theory calculations to investigate how the O 1s binding energy in CeO₂(111) is influenced by the presence of oxygen vacancies. The case with point vacancies in CeO₂(111) is compared to complete reduction to Ce₂O₃. Reduction of CeO₂ by oxygen vacancies is found to have a minor effect on the O 1s binding energy. The O 1s binding energy is instead clearly changed when the character of the chemical bond for the considered oxygen atom is modified by, for example, the formation of OH-groups or carbonates.

Keywords: ceria, XPS, DFT, oxygen vacancies

(Some figures may appear in colour only in the online journal)

1. Introduction

Physical and chemical properties of oxide surfaces may depend strongly on the presence of oxygen vacancies. For reducible oxides such as CeO₂, oxygen vacancies create occupied states in the band-gap, which modifies optical and catalytic properties [1]. Thus, to establish structure-function relationships, it is desirable to know if vacancies are present. X-ray photoemission spectroscopy (XPS) is the standard technique for chemical analysis [2], which has been used to make conclusions regarding the presence of vacancies in different oxides by measuring shifts in O 1s binding energy, see e.g. references [3–7]. The assigned shift is commonly about 1–2 eV

to higher binding energies than the O 1s binding energy in the bulk oxide. The assignment of shifts in O 1s binding energies to oxygen vacancies is based on the assumption that the presence of vacancies changes the electrostatic potential for the oxygen anions that are left in the system.

Core level shifts (CLS) of O 1s has also been used to make conclusions regarding oxygen vacancies in CeO₂. For CeO₂, vacancy induced shifts have been reported in the range from 1 to 2.5 eV [8–13]. For example, in reference [10], the interaction of oxidized and partially reduced CeO₂ with water was studied by a range of techniques including synchrotron-radiation photoelectron spectroscopy. The O 1s binding energy for oxygen atoms in the bulk of CeO_{2-x} (with $x = 0.16$) was measured to be 529.7 eV. An O 1s binding energy feature at 532.0 eV was for this system assigned to oxygen atoms close to Ce³⁺, resulting in a shift of 2.3 eV.

It should be noted that the literature on shifts of the O 1s binding energies in the presence of oxygen vacancies is not consistent and measurements have also been reported with no

* Authors to whom any correspondence should be addressed.



Original content from this work may be used under the terms of the [Creative Commons Attribution 4.0 licence](https://creativecommons.org/licenses/by/4.0/). Any further distribution of this work must maintain attribution to the author(s) and the title of the work, journal citation and DOI.

or minor shifts [14–18]. Early studies measured a shift of only 0.3 eV for vacancies in CeO_2 [14] and, similarly, a small shift of 0.2 eV between CeO_2 and the fully reduced phase Ce_2O_3 has been reported [15]. In reference [18], the reduction of a $\text{CeO}_2(111)/\text{Ru}(0001)$ surface by atomic hydrogen was investigated by means of scanning tunneling microscopy and x-ray photoelectron spectroscopy. Exposing the sample to atomic hydrogen resulted initially to the formation of OH trimers and eventually to H_2O formation and desorption leading to oxygen vacancies. The presence of oxygen vacancies did not result in additional peaks in the O 1s spectrum although signatures of the vacancies were visible in the Ce 3d spectrum [18].

We have recently studied the effect of oxygen vacancies on O 1s CLS for different oxides including $\text{CeO}_2(111)$ [19] using density functional theory (DFT) calculations. The calculations did not reveal any O 1s shift owing to vacancies. However, the calculations were restricted to point defects in the most stable surfaces without the possibility of structural transformations, which could induce changes in the Madelung potential and, thus, a possible shifts in the O 1s binding energy.

The unclear situation without a consensus whether signatures of oxygen vacancies are visible in the O 1s core level spectrum of reduced ceria have motivated us to further explore the issue with DFT calculations. Here we consider O 1s CLS for $\text{CeO}_2(111)$, $\text{CeO}_2(111)$ with vacancies and $\text{Ce}_2\text{O}_3(0001)$ together with hydroxyl- and carbonate-groups on $\text{CeO}_2(111)$. We find that vacancies are not visible as shifts in the O 1s spectrum. Chemical reasons for observed shifts could instead be the presence of contaminants giving rise to hydroxyl- and carbonate-groups.

2. Computational method

The Vienna *ab initio* Simulation Package [20–23] was used to perform DFT calculations. The plane augmented wave (PAW) method [24, 25] was used to model the interaction between the valence electrons and the cores. Electrons treated in the valence were $1s^1$ for H, $2s^22p^2$ for C, $2s^22p^4$ for O and $5s^25p^65d^14f^16s^2$ for Ce. The exchange–correlation functional according to Perdew, Burke and Ernzerhof [26] augmented with a Hubbard-U correction for Ce 4f states [27] was used to account for exchange and correlation effects. The Hubbard-U correction is required to localize the Ce 4f states and we used a value of 4.5 eV, which has been used previously [28]. The Kohn–Sham orbitals were expanded with plane waves using a 450 eV cut-off. A Monkhorst–Pack scheme [29, 30] was used to generate k -points for a numerical integration over the Brillouin zone. Slabs of $\text{CeO}_2(111)$ and $\text{Ce}_2\text{O}_3(0001)$ were considered and the repeated slabs were separated by at least 15 Å of vacuum. All structures were optimized using the method of conjugate gradients until the largest force was smaller than $0.03 \text{ eV } \text{\AA}^{-1}$.

The CLS were calculated as total energy differences with a core hole either in the surface or in the center of the slab. This method includes complete screening of the core hole [31] and is based on the assumptions that the photo-emission process is fast with respect to the lifetime of the core hole, that the system remains in the ground state (with the constraint of

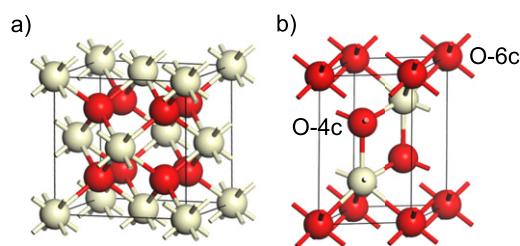


Figure 1. (a) CeO_2 bulk structure. (b) Ce_2O_3 bulk structure. The four- and six-fold coordination of the oxygen atoms are indicated for Ce_2O_3 . Atomic color codes: Ce (beige) and O (red).

a core hole), and that structural changes are small. The core holes were obtained by removing one electron from the O 1s shell in the PAW potential.

The presence of a core hole means that the system is ionized. However, periodic boundary conditions requires neutral supercells. The charge neutrality could be maintained either by adding an extra electron to the valence or by applying a compensating jellium background. The addition of an extra electron could be done for metallic systems, where the character of the occupied and unoccupied states are similar [32]. As ceria has a band gap, the CLS were here calculated by the use of a negatively charged homogeneous jellium background.

3. Results

3.1. Structural models

The considered bulk structures are shown in figure 1. The bulk structure of CeO_2 is of fluorite type, with four Ce^{4+} cations and eight O^{2-} anions. The four Ce^{4+} cations are eight-fold coordinated, whereas the oxygen are four-fold coordinated. The optimized lattice parameter is $a = 5.49 \text{ \AA}$, which agrees with previous DFT studies [1, 33] and the experimental value of 5.41 \AA . Ce_2O_3 has an hexagonal structure with two Ce^{4+} cations and three O^{2-} anions. The two cerium atoms are seven-fold coordinated. Two of the oxygen atoms are four-fold coordinated, whereas the third oxygen atom is six-fold coordinated. The optimized lattice parameters are $a = b = 3.92 \text{ \AA}$ and $c = 6.16 \text{ \AA}$, which agrees with previous DFT-reports [34, 35]. The experimental lattice parameters are $a = b = 3.89 \text{ \AA}$ and $c = 6.06 \text{ \AA}$.

One important difference between stoichiometric and reduced ceria is that the 4f-states are partially occupied for Ce_2O_3 . The density of states (DOS) for the two bulk structures are shown in figure 2. The oxidation state of the cerium atoms in CeO_2 is +4, meaning that the 4f states are empty. In the DOS, the empty 4f-states are 2.2 eV above the Fermi energy. The states below the Fermi energy are of O 2p character. The 4f-states become occupied for Ce_2O_3 , forming states at the Fermi energy. The occupation of 4f-states is linked with a change in the oxidation state of the cerium atoms from +4 to +3. The occupied 4f-states are split from the unoccupied 4f-states, which are located about 2.4 eV above the Fermi energy. The O 2p states are for Ce_2O_3 located in a range from -4.4 eV to -1.6 eV below the Fermi energy.

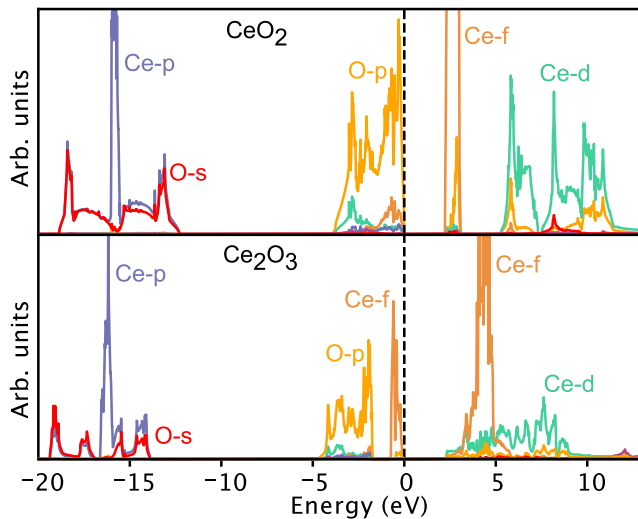


Figure 2. Projected DOS for bulk CeO_2 (top) and Ce_2O_3 (bottom). The energy is given with respect to the Fermi energy.

The stable surfaces for stoichiometric and reduced ceria are $\text{CeO}_2(111)$ and $\text{Ce}_2\text{O}_3(0001)$, respectively. $\text{CeO}_2(111)$ is modeled with a (3×3) supercell with five O–Ce–O layers. The top most oxygen atoms are three-fold coordinated, whereas the oxygen atoms in the bulk are four-fold coordinated. $\text{Ce}_2\text{O}_3(0001)$ is modeled with a (3×3) cell with three O–Ce–O–Ce–O layers. Also in this case, the surface has three-fold coordinated oxygen atoms, whereas the oxygen atoms in the bulk are either four- or six-fold coordinated.

In addition to the pristine $\text{CeO}_2(111)$ and $\text{Ce}_2\text{O}_3(0001)$ surfaces, we have modeled a $\text{CeO}_2(111)/\text{Ce}_2\text{O}_3(0001)$ interface. This model makes it possible to directly compare the O 1s CLS for stoichiometric and reduced ceria. The interface model is modeled with four tri-layer of $\text{CeO}_2(111)$ merged with two penta-layers of $\text{Ce}_2\text{O}_3(0001)$. Thus, the interface model preserves the stoichiometry of the two oxides. The interface model is constructed with the in-plane lattice constant of CeO_2 , giving a slight compression (1%) of the Ce_2O_3 layers. The model structures are shown in figure 3.

CeO_2 is a closed-shell electronic system in the absence of vacancies. When vacancies are formed, electrons occupy the 4f-states in a ferromagnetic (FM) or anti-ferromagnetic (AFM) fashion. The FM and AFM solutions for $\text{CeO}_2(111)$ with vacancies are in our calculations close to degenerate. For $\text{Ce}_2\text{O}_3(0001)$, the AFM configuration is preferred with alternating spin-up and spin-down Ce^{3+} layers. The magnetic ordering was obtained by analyzing the magnetization.

3.2. O 1s core level shifts for the surface models

To investigate the possibility to measure shifts in the O 1s binding energies between pristine CeO_2 , partially or completely reduced CeO_2 , we calculated O 1s CLS for $\text{CeO}_2(111)$, $\text{CeO}_2(111)$ with oxygen vacancies, $\text{Ce}_2\text{O}_3(0001)$ and the interface system. The shifts are calculated as the total energy difference between the system with a core-hole in the atom of interest and a core-hole in the bulk. The atoms that are selected

to represent the bulk are shown in figure 3. A CeO_2 -reference is chosen for the interface model (C). The results are presented in table 1.

The shifts for surface oxygen atoms in both $\text{CeO}_2(111)$ and $\text{Ce}_2\text{O}_3(0001)$ are negative. For $\text{CeO}_2(111)$, the shift for the top most oxygen atoms are -0.47 eV, whereas the sub-surface atoms have shifts of only -0.02 eV. The surface CLS is only slightly affected by the presence of an oxygen vacancy. In $\text{Ce}_2\text{O}_3(0001)$, the oxygen atoms have different coordination, being either four or six-fold coordinated. The reference is in this case considered to be an average between four- and six-fold coordinated bulk atoms. The O 1s binding energy of the two types of atoms differ by 0.19 eV. The CLS for a surface atom in $\text{Ce}_2\text{O}_3(0001)$ is calculated to be -0.17 eV, whereas the sub-surface atoms have a shift of -0.14 eV. The smaller CLS for $\text{Ce}_2\text{O}_3(0001)$ as compared to $\text{CeO}_2(111)$ is consistent with previous calculations for irreducible oxides such as $\text{MgO}(100)$, which show small negative shifts [19].

For the interface system (C), the CLS have been calculated with respect to the bulk of the $\text{CeO}_2(111)$ slab, as shown in figure 3. The shifts for surface atoms of the $\text{Ce}_2\text{O}_3(0001)$ part are positive, being 0.34 eV and 0.29 eV for the surface and sub-surface atoms, respectively. Thus, for this system where ceria is completely reduced (maximum number of vacancies), the shifts in O 1s binding energies are clearly smaller than the experimentally assigned shifts of 1–2.5 eV [8–13].

One important contribution to the CLS is the electronic screening where the creation of the core-hole attracts additional charge to the core-excited atom. We have investigated the screening by performing a Bader charge analysis [36]. The charge on the anions of $\text{CeO}_2(111)$ is calculated to be $\simeq 7.2$ electrons, whereas the charge on a core excited atom is about 7.8 electrons. Thus, the core hole attracts 0.6 electrons. The Bader analysis for $\text{Ce}_2\text{O}_3(0001)$ shows a charge of $\simeq 7.35$ electrons. The corresponding charge in the presence of a core-hole is 7.9 electrons. In this case, the core-hole attracts about 0.5 electrons. The Bader charges for the interface system are consistent with the results for the pristine surfaces. As the $2s^2 2p^6$ configuration of an oxygen anion constitutes a closed shell, this is also the formal screening configuration for a core excited oxygen atom in an oxide. The reason why the charge screening for reduced ceria is lower than for the stoichiometric case is that the oxygen anions in Ce_2O_3 are closer to the $2s^2 2p^6$ configuration in the unexcited state.

3.3. Effects of adsorbates

As oxygen vacancies do not result in large positive shifts, we have studied whether the observed experimental CLS could originate from different adsorbates on stoichiometric ceria. The reference atom is in this case a bulk CeO_2 atom, as for the pristine model system A. The considered adsorbates are OH groups produced by dissociated H_2 , water and adsorbed CO_2 forming CO_3^{2-} . The considered structures and the corresponding CLS are shown in figure 4.

The presence of oxygen vacancies results in the change of oxidation state of two cerium atoms. The stable configuration

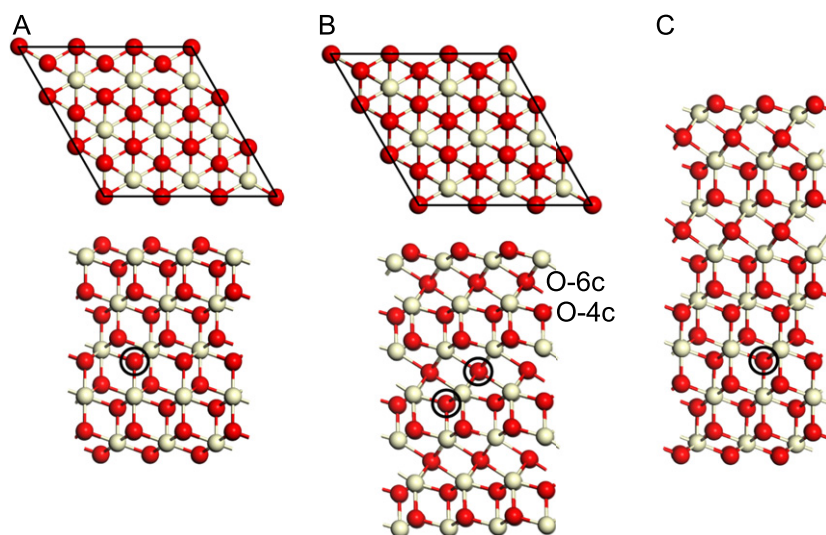


Figure 3. (A) Top and side view of $\text{CeO}_2(111)$. (B) Top and side view of $\text{Ce}_2\text{O}_3(0001)$ with the four- and six-fold coordination of the oxygen atoms indicated. (C) Side view of the $\text{CeO}_2(111)/\text{Ce}_2\text{O}_3(0001)$ interface model. The interface model is constructed with the $\text{Ce}_2\text{O}_3(0001)$ slab placed on-top of the $\text{CeO}_2(111)$ slab. The considered surface cells are indicated for $\text{CeO}_2(111)$ and $\text{Ce}_2\text{O}_3(0001)$. Atomic color codes: Ce (beige) and O (red). The circles indicate atoms that have been selected as bulk references in the calculation of the CLS. A CeO_2 -reference is chosen for the interface model.

Table 1. O 1s surface CLS for the considered systems. The reference atoms for the CLS are shown in figure 3. Note that the shift for model B is calculated with respect to a bulk atom in Ce_2O_3 , whereas the shifts for model C are calculated with respect to a bulk atom in CeO_2 . c and c_{screened} are the calculated atomic charges for the considered oxygen atom without and with core-hole, respectively.

	Model	Site	CLS	c	c_{screened}
$\text{CeO}_2(111)$	A	Surf.	−0.47	7.19	7.82
$\text{CeO}_2(111)$	A	Sub-surf.	−0.02	7.20	7.85
$\text{CeO}_2(111)$	A	Surf. vac.	−0.30	7.22	7.80
$\text{Ce}_2\text{O}_3(0001)$	B	Surf.	−0.17	7.34	7.88
$\text{Ce}_2\text{O}_3(0001)$	B	Sub-surf.	−0.14	7.40	7.89
$\text{CeO}_2(111)$	C	Surf.	−0.57	7.19	7.79
$\text{CeO}_2(111)$	C	Sub-surf.	−0.08	7.20	7.81
$\text{Ce}_2\text{O}_3(0001)$	C	Surf.	0.34	7.32	7.82
$\text{Ce}_2\text{O}_3(0001)$	C	Sub-surf.	0.29	7.40	7.86

in presence of a vacancy corresponds to Ce^{3+} atoms in next nearest neighbor position with respect to the vacancy [37]. The presence of OH groups is investigated with H_2 dissociated in an homolytic fashion. The adsorption of OH groups also leads to the formations of two Ce^{3+} atoms. The adsorption energy is -1.17 eV per H, which is in agreement with previous results [38].

Water can on $\text{CeO}_2(111)$ coexist in molecular form and as a hydroxyl-pair [39]. The two OH-groups are bonded through a hydrogen bond in the hydroxyl-pair. The adsorption energy of the hydroxyl-pair is calculated to be -0.56 eV. Molecular water is adsorbed with an adsorption energy of -0.53 eV, which agrees with previous work [39]. The adsorption energy of CO_2 forming a carbonate is -0.61 eV, which also agrees with previous work [40].

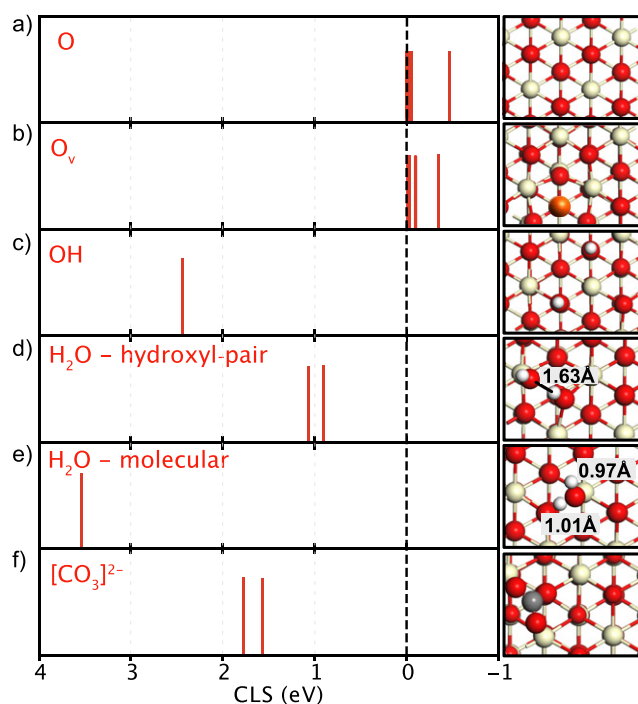


Figure 4. Left: core level shift for different structures and adsorbate on $\text{CeO}_2(111)$. Right: the corresponding structure. (a) Pristine $\text{CeO}_2(111)$, (b) $\text{CeO}_2(111)$ with oxygen vacancy, (c) OH groups from dissociated H_2 , (d) OH groups in the hydroxyl pair, (e) molecular water, (f) adsorbed CO_2 . Atomic color code: Ce (beige), O (red), O vacancy (orange), H (white), C (dark gray).

The calculated CLS shows that the shift for the oxygen vacancy is close to the shift for the pristine case, suggesting that such shift is difficult to observe in an XPS experiment. On the contrary, the O 1s shift for the OH group is 2.44 eV and the

shift from water in the form of the hydroxyl-pair, is between 0.97 and 1.07 eV. The calculated shifts agree with experimental results where a O 1s shift around 1.75 eV was assigned to the presence of OH groups, and a shift around 3.2 eV was assigned to molecular water [41].

The difference between the shifts of the OH groups formed by H₂ dissociation and water in hydroxyl pair form, originates from the presence of a hydrogen bond between the OH groups. In fact, when the OH group on a cerium atom is placed far from the lattice OH group, the shift increases from about 1 eV to about 2 eV. The carbonate structure results in two CLS at 1.57 eV and 1.78 eV, respectively. The larger shift corresponds to the oxygen atom in the lattice.

The O 1s CLS obtained for OH and carbonate adsorbates could potentially explain the experimental shifts attributed to oxygen vacancies. Our calculations agree with experimental literature where minor shifts have been attributed to oxygen vacancies, and instead pronounced shifts have been attributed to OH groups [14–18, 41]. The calculated shifts for OH-groups are in the range where assignments have been done to oxygen vacancies [8–13].

4. Conclusions

We have used DFT calculations to investigate O 1s CLS for CeO₂(111) with the goal to elucidate whether oxygen vacancies result in measurable shifts. The origin of measured O 1s shifts is important when establishing structure-function relationships. The pristine surface was investigated together with CeO₂(111) including vacancies, completely reduced Ce₂O₃(0001) and hydroxyl- and carbonate-groups on CeO₂(111). We do not find any substantial O 1s shifts related to reduced ceria. Clear shifts are instead calculated in the presence of adsorbates. Experimentally, shifts in the O 1s binding energy of 1–2.5 eV have previously been assigned to oxygen atoms coordinated to Ce³⁺ formed by the presence of oxygen vacancies. Our calculations indicate that such shifts instead could be due to contaminations, such as H₂, H₂O and CO₂.


Acknowledgments

Financial support from the Knut and Alice Wallenberg Foundation through the project ‘Atomistic design of catalysts’ (No: KAW 2015.0058) and the Swedish Research Council (2020-05191) is gratefully acknowledged. The calculations have been performed at C3SE (Göteborg) and PDC (Stockholm) through a SNIC Grant. The Competence Centre for Catalysis is hosted by Chalmers University of Technology and financially supported by the Swedish Energy Agency and the member companies AB Volvo, ECAPS AB, Johnson Matthey AB, Preem AB, Scania CV AB, and Umicore Denmark Aps.

Data availability statement

The data generated and/or analysed during the current study are not publicly available for legal/ethical reasons but are available from the corresponding author on reasonable request.

ORCID iDs

Andreas Schaefer  <https://orcid.org/0000-0001-6578-5046>
Henrik Grönbeck  <https://orcid.org/0000-0002-8709-2889>

References

- [1] Skorodumova N V, Ahuja R, Simak S I, Abrikosov I A, Johansson B and Lundqvist B I 2001 *Phys. Rev. B* **64** 115108
- [2] Siegbahn K 1982 *Rev. Mod. Phys.* **54** 709
- [3] Fan J C C and Goodenough J B 1977 *J. Appl. Phys.* **48** 3524–31
- [4] Zhang X, Qin J, Xue Y, Yu P, Zhang B, Wang L and Liu R 2014 *Sci. Rep.* **4** 4596
- [5] Fang J, Fan H, Ma Y, Wang Z and Chang Q 2015 *Appl. Surf. Sci.* **332** 47–54
- [6] Pilz J, Perrotta A, Christian P, Tazreiter M, Resel R, Leising G, Griesser T and Coclite A M 2018 *J. Vac. Sci. Technol. A* **36** 01A109
- [7] Frei M S *et al* 2019 *Nat. Commun.* **10** 3377
- [8] Holgado J P, Munuera G, Espinós J P and González-Elipe A R 2000 *Appl. Surf. Sci.* **158** 164–71
- [9] Natile M M and Glisenti A 2006 *Surf. Sci. Spectra* **13** 17–30
- [10] Lykhach Y *et al* 2012 *J. Phys. Chem. C* **116** 12103–13
- [11] Hasegawa T, Shahed S M F, Sainoo Y, Beniya A, Isomura N, Watanabe Y and Komeda T 2014 *J. Chem. Phys.* **140** 044711
- [12] Barth C, Laffon C, Olbrich R, Ranguis A, Parent P and Reichling M 2016 *Sci. Rep.* **6** 21165
- [13] Shah P M, Burnett J W H, Morgan D J, Davies T E and Taylor S H 2019 *Catalysts* **9** 475
- [14] Mullins D R, Overbury S H and Huntley D R 1998 *Surf. Sci.* **409** 307–19
- [15] Praline G, Koel B E, Hance R L, Lee H-I and White J M 1980 *J. Electron Spectrosc. Relat. Phenom.* **21** 17–30
- [16] Wilkens H *et al* 2013 *Phys. Chem. Chem. Phys.* **15** 18589–99
- [17] Pereira A, Blouin M, Pillonnet A and Guay D 2014 *Mater. Res. Express* **1** 15704
- [18] Shahed S M F, Hasegawa T, Sainoo Y, Watanabe Y, Isomura N, Beniya A, Hirata H and Komeda T 2014 *Surf. Sci.* **628** 30–5
- [19] Posada-Borbón A, Bosio N and Grönbeck H 2021 *Surf. Sci.* **705** 121761
- [20] Kresse G and Hafner J 1993 *Phys. Rev. B* **47** 558
- [21] Kresse G and Hafner J 1993 *Phys. Rev. B* **49** 14251
- [22] Kresse G and Furthmüller J 1996 *Comput. Mater. Sci.* **6** 15
- [23] Kresse G and Furthmüller J 1996 *Phys. Rev. B* **54** 11169
- [24] Blöchl P E 1994 *Phys. Rev. B* **50** 17953
- [25] Kresse G and Joubert D 1999 *Phys. Rev. B* **59** 1758
- [26] Perdew J P, Burke K and Ernzerhof M 1996 *Phys. Rev. Lett.* **77** 3865
- [27] Dudarev S L, Botton G A, Savrasov S Y, Humphreys C J and Sutton A P 1998 *Phys. Rev. B* **57** 1505–9
- [28] Huang M and Fabris S 2008 *J. Phys. Chem. C* **112** 8643–8
- [29] Monkhorst H J and Pack J D 1976 *Phys. Rev. B* **13** 5188
- [30] Pack J D and Monkhorst H J 1977 *Phys. Rev. B* **16** 1748
- [31] Pehlke E and Scheffler M 1993 *Phys. Rev. Lett.* **71** 2338
- [32] Van den Bossche M, Martin N M, Gustafson J, Hakanoglu C, Weaver J F, Lundgren E and Grönbeck H 2014 *J. Chem. Phys.* **141** 034706

- [33] Andersson D A, Simak S I, Johansson B, Abrikosov I A and Skorodumova N V 2007 *Phys. Rev. B* **75** 035109
- [34] Da Silva J L F 2007 *Phys. Rev. B* **76** 193108
- [35] Matz O and Calatayud M 2019 *Top. Catal.* **62** 956–67
- [36] Bader R 1990 *Atoms in Molecules: A Quantum Theory* (New York: Oxford University Press)
- [37] Ganduglia-Pirovano M V, Da Silva J L F and Sauer J 2009 *Phys. Rev. Lett.* **102** 026101
- [38] Fernández-Torre D, Carrasco J, Ganduglia-Pirovano M V and Pérez R 2014 *J. Chem. Phys.* **141** 014703
- [39] Fernández-Torre D, Košmider K, Carrasco J, Ganduglia-Pirovano M V and Pérez R 2012 *J. Phys. Chem. C* **116** 13584–93
- [40] Baumann N, Lan J and Iannuzzi M 2021 *J. Chem. Phys.* **154** 094702
- [41] Carrasco J *et al* 2015 *Angew. Chem., Int. Ed.* **54** 3917–21